

## Exploring suitable domain size for high-resolution urban rainfall simulation

Sichan Du <sup>a,\*</sup>, Lu Zhuo <sup>a,b</sup>, Elizabeth J. Kendon <sup>c,d</sup>, Dawei Han <sup>a</sup>

<sup>a</sup> Department of Civil Engineering, University of Bristol, Bristol BS8 1TR, UK

<sup>b</sup> School of Earth and Environmental Sciences, Cardiff University, Cardiff CF10 3AT, UK

<sup>c</sup> Met Office Hadley Centre, FitzRoy Road, Exeter EX1 3PB, UK

<sup>d</sup> School of Geographical Sciences, University of Bristol, Bristol BS8 1SS, UK

### ARTICLE INFO

#### Keywords:

Urban rainfall simulation  
High-resolution model performance  
Suitable domain size (SDS)  
Weather research and forecasting (WRF) model  
Newcastle upon Tyne

### ABSTRACT

High-resolution urban rainfall simulation is useful for understanding the interaction between urbanisation and local weather as well as the impact of climate change over cities and the impact of adaptation measures such as urban greening. Previous studies on mesoscale Numerical Weather Prediction (NWP) modelling have largely focused on spatial resolution and other aspects (e.g., spin-up time and model parameterisations), with limited investigations on how to determine a suitable domain size. Domain size is likely an important factor when the spatial resolution of modelling is within convection-permitting regime (less than 5 km). In this study, 64 summer domain tests are simulated with the Weather Research and Forecasting (WRF) model, over Newcastle upon Tyne, with ERA5 as input data and a radar product from the UK Met Office for validation. Using an integrated evaluation indicator, alongside spatial distribution maps, it has been found that too large or too small domain sizes both have negative impacts on the simulation results and an optimal domain size for the events here is identified. We find that domain size has a stronger influence on the event simulation than changing grid resolution within the range 1–4.5 km and thus should be a primary consideration. We also find that, for more accurate simulation, smaller domain sizes are better suited to heavy rainfall events than to lighter ones. In a similar way, smaller domain sizes perform better for rainfall events that cover larger spatial areas. Although the optimal domain size identified here is specific to the region/season, the sensitivities and relative influences are expected to be more generally applicable and show the importance of testing domain sizes before embarking on production simulations.

## 1. Introduction

With the trend of global urban growth, research on cities related to the urban hydrometeorological environment becomes increasingly important (Shepherd, 2005). Urbanisation can directly influence the natural environment by impacting the local climate, including the well-known Urban Heat Island (UHI) effect, as well as its influence on precipitation. Observational and modelling studies suggest that urban areas may amplify and modify precipitation patterns, convective storms, and flood events (Mitra and Shepherd, 2015), and this remains an active area of research. Cities are particularly vulnerable to flash flooding due to impermeable surfaces, and

\* Corresponding author.

E-mail addresses: [sichan.du@bristol.ac.uk](mailto:sichan.du@bristol.ac.uk) (S. Du), [zhuol@cardiff.ac.uk](mailto:zhuol@cardiff.ac.uk) (L. Zhuo), [elizabeth.kendon@metoffice.gov.uk](mailto:elizabeth.kendon@metoffice.gov.uk) (E.J. Kendon), [d.han@bristol.ac.uk](mailto:d.han@bristol.ac.uk) (D. Han).

<https://doi.org/10.1016/j.uclim.2025.102489>

Received 7 October 2024; Received in revised form 15 April 2025; Accepted 31 May 2025

Available online 5 June 2025

2212-0955/Crown Copyright © 2025 Published by Elsevier B.V. This is an open access article under the CC BY license (<http://creativecommons.org/licenses/by/4.0/>).

with climate change, the frequency and intensity of extreme rainfall are expected to increase, potentially exacerbated by urbanisation (Shepherd et al., 2002; Pachauri et al., 2014; Stocker, 2014). Understanding the detailed spatio-temporal precipitation patterns over urban areas is crucial for designing future climate-resilient cities (Seto et al., 2012; Manola et al., 2020; Jong et al., 2023), in which Numerical Weather Prediction (NWP) modelling plays an important role.

Many studies on NWP modelling have examined the impacts of model resolutions on rainfall simulation performance. According to Sun and Ao (2013), Kim et al. (2019) as well as Xie and Wang (2021), model resolution was recognised as a key factor influencing rainfall simulation accuracy. Xu et al. (2017) and Bonekamp et al. (2018) showed that coarse resolutions struggled to capture the processes and features at an urban scale, particularly for the rainfall events occurring in complex terrains (Ménégoz et al., 2013; Liu et al., 2018; Schneider et al., 2018; Duan et al., 2019). Some studies also suggested that higher resolution enhances simulation performance for urban rainfall (Kharin et al., 2013; Xie et al., 2015; Pfahl et al., 2017), but precipitation properties (e.g., rainfall amount and rainfall spatial coverage) must also be considered (Mahoney et al., 2013; Feng et al., 2018; Vanden Broucke et al., 2019; Jin et al., 2023). Ochoa-Rodriguez et al. (2015) concluded that a resolution around 1 km is generally sufficient for urban research, while Fossier et al. (2020) argued that convection-permitting resolutions (less than 5 km) are necessary to accurately capture convective rainfall.

In comparison with model resolutions within the convection-permitting regime, domain size is another crucial factor in high-resolution modelling that has received relatively less attention. Whereas, the high computational costs of high-resolution simulations often constrain domain sizes, which may introduce additional uncertainties and errors in weather forecasting. Leduc and Laprise (2009) employed a “perfect model” approach on domain size research in the context of regional climate modelling and argued that too large and too small domain sizes should be avoided. Goswami et al. (2012) simulated three rainfall events to explore model performance and found that the influence of domain size on the results was as important as that of grid resolution and initial conditions (Wang et al., 2016), impacting metrics such as Total Cumulative Rainfall (TCR) and Hourly Maximum Rainfall (HMR). As far as Giorgi and Mearns (1999) were concerned, the selection of domain size is crucial for mesoscale simulation, however, there are no universal criteria for its choice because of variations in regional characteristics and experiment design. Consequently, trial-and-error remains a commonly used method in domain size selection, but some studies have increasingly adopted more systematic approaches, such as sensitivity experiments, performance-based evaluations or physical reasoning, to identify suitable domain configurations (Bhaskaran et al., 2012; Qian and Zubair, 2010; Dash et al., 2015). Such investigations highlight the need for more generalisable and robust guidelines for domain size determination across models and regions.

The Weather Research and Forecasting (WRF) model, known for its effectiveness in simulating regional domains with high resolutions, is particularly suited for urban rainfall simulation. For the method on selecting domain size, the normal way is under nested scenario (with multiple domains): determining the finest grid resolution to be explored, utilising an appropriate parent\_grid\_ratio (recommended ratios are 3 or 5), employing a certain number of grid point (for parent domain and nested domain, respectively). Then, each domain size could be confirmed. Our research’s novelty is on the method by setting the coarsest domain size (single domain) under different configurations on grid resolution and grid point, along with eliminating the interference of grid resolution on the WRF simulation.

In this study, we investigate the Suitable Domain Size (SDS, the domain size with the best simulated result) for the WRF high-resolution rainfall simulation in a UK city—Newcastle upon Tyne (hereafter “Newcastle”). Using an objective method, we aim to determine acceptable SDS ranges (the range of several domain sizes with better simulated results for each rainfall event), identify a common optimal SDS (the domain size that performs reliably across multiple urban rainfall events), and explore the relationship between domain size and rainfall characteristics by considering the former as a variable influenced by factors such as rainfall amount and rainfall spatial coverage (Sofokleous et al., 2021). We simulate eight rainfall events in Newcastle over the past 13 years under eight different domain sizes using the WRF model. Our research questions are:

- 1) What are the acceptable SDS ranges for varied rainfall events?
- 2) Can we identify a common optimal SDS?
- 3) How do acceptable SDS ranges vary with rainfall amount and rainfall spatial coverage?

After the introduction in Section 1, Section 2 presents the data (target city and selected database) and methods (model configuration, event setting, and WRF evaluation) related to this research. Section 3 provides the experimental results, followed by an expanded discussion in Section 4. Finally, Section 5 addresses the research questions and discusses the implications for future research.

## 2. Data and methods

### 2.1. Preparatory work

#### 2.1.1. Study area

Newcastle is the largest city in North East England, located on the northern bank of the River Tyne, approximately 13.7 km from the North Sea (Wikimedia Foundation, 2022). It lies within the Tyne Valley, flanked by the Pennines to the west and coastal plains to the east. This transitional topography, combined with its maritime climate and dense urbanisation, makes it particularly sensitive to convective rainfall events (bluegreencities, 2013). Fig. 1 depicts the location (54.9783° N, 1.6178° W) and outline (in yellow) of Newcastle in Google Earth Pro. Due to the 92 % impermeable surface in the city centre, Newcastle is prone to urban flooding, particularly during intense rainfall when local drainage systems are overwhelmed. Newcastle is equipped with numerous sensors that gather data across the city, which facilitates meteorological data acquisition (urbanobservatory, 2016). The dense population and



**Table 1**  
WRF basic settings for rainfall events.

Variables	Settings
Map Projection	Lambert
Central Point of Domain	Latitude: 54.98 Longitude: -1.62
Latitudinal Grid Length & Longitudinal Grid Length	Regional Convection-Permitting Resolutions (1 km–4.5 km, Resolution Interval: 0.5 km)
Model Output Time Step	Hourly
Nesting State	Single Model Domain
West-East Dimension & South-North Dimension	100 × 100
Pressure Top	5000 Pa
Vertical Levels	58
Simulation Period (HH:MM, DD/MM/YYYY)	00:00, 19/08/2021 to 23:00, 22/08/2021 00:00, 25/08/2020 to 23:00, 28/08/2020 00:00, 09/06/2020 to 23:00, 12/06/2020 00:00, 11/06/2019 to 23:00, 14/06/2019 00:00, 05/06/2017 to 23:00, 08/06/2017 00:00, 10/06/2016 to 23:00, 13/06/2016 00:00, 04/06/2014 to 23:00, 07/06/2014 00:00, 15/07/2011 to 23:00, 18/07/2011

## 2.2. Experimental design

### 2.2.1. WRF general settings

As one of the most widely used NWP models worldwide (National Center for Atmospheric Research, 2004; Cheng et al., 2013; Powers et al., 2017; Cui et al., 2019; Hewage et al., 2021), the WRF model possesses a variety of functions for a broad range of applications. The WRF model is an atmospheric model and includes dynamical solvers and physics packages, for atmospheric processes containing microphysics, radiation, planetary boundary layer, etc. (Skamarock et al., 2008). The WRF Preprocessing System (WPS) pulls in geographical information and sets up model domains, followed by taking in, reformatting and interpolating atmospheric data to user's domains.

The general settings of the WRF model (version 4.3) used here for simulating eight Newcastle rainfall events occurring over the past 13 years, from 2011 to 2021, are shown in Table 1. We utilise resolutions within the convection-permitting regime (grid resolution between 1 km and 4.5 km with an increment of 0.5 km). Hourly model outputs are compared with the observation data. The model is driven by ERA5 at its lateral boundaries (Wang and Gill, 2012). Domain size is varied in sensitivity experiments, but an initial configuration of 100 grid points along West-East and South-North dimensions is selected for each event, as recommended in the best practice of the WRF official guidance (National Center for Atmospheric Research, 2016a). For the pressure top and the number of vertical levels used in the model, their values are suggested from WRF user manual (National Center for Atmospheric Research, 2016b). The simulation period for the eight rainfall events is four days, including the first day as the spin-up period. Liu et al. (2023) confirmed that 24 h can be the minimum time span to obtain a relatively accurate and computationally efficient simulation result by the WRF model, because it allows the model to adequately adjust from the initial conditions to a dynamically balanced state. By ensuring that atmospheric processes have stabilised, the model could produce more reliable rainfall predictions (Deng and Stauffer, 2006; Skamarock et al., 2008). The physics options used here are shown in Table 2 (National Center for Atmospheric Research, 2021).

### 2.2.2. Specific settings for rainfall events

To determine the optimal SDS within the convection-permitting regime, eight cases, each with varying domain sizes, were run by the WRF model for eight Newcastle rainfall events, respectively (i.e., in total, there are  $8 \times 8 = 64$  simulations). ERA5 data were

**Table 2**  
WRF physics options.

Section	Physics Option	Code Number	Reference
Micro Physics (mp_physics)	Thompson Scheme	8	(Thompson et al., 2008)
Planetary Boundary Layer (PBL) Physics (bl_pbl_physics)	Mellor–Yamada–Janjic (MYJ) Scheme	2	(Mesinger, 1993; Janjic, 1994)
Cumulus Parameterisation (cu_physics)	Betts–Miller–Janjic Scheme	2	(Janjic, 1994)
Shortwave (ra_sw_physics) and Longwave (ra_lw_physics)	Dudhia Shortwave Scheme	1	(Dudhia, 1989)
Land Surface (sf_surface_physics)	RRTM Longwave Scheme	1	(Mlawer et al., 1997)
Surface Layer (sf_sfclay_physics)	Unified Noah Land Surface Model	2	(Tewari et al., 2004)
Urban Surface (sf_urban_physics)	Eta Similarity Scheme	2	(Monin and Obukhov, 1954; Janjic, 1994; Janjic, 1996; Janjic, 2001)
	Building Environment Parameterization (BEP) Scheme	2	(Martilli et al., 2002; Salamanca and Martilli, 2010)

**Table 3**  
Single model domain settings for each rainfall event.

Newcastle Rainfall	Grid Resolution (km)	Time Step (s)	Grid Point	Domain Size (km <sup>2</sup> )
case 1	4.5	<b>25</b>	100	450 × 450
case 2	4	24	100	400 × 400
case 3	3.5	<b>20</b>	100	350 × 350
case 4	3	18	100	300 × 300
case 5	2.5	15	100	250 × 250
case 6	2	12	100	200 × 200
case 7	1.5	9	100	150 × 150
case 8	1	6	100	100 × 100

downscaled directly from 31 km to the grid resolutions listed in Table 3 without an intermediate nest. The significant resolution jump from ERA5 (31 km) to WRF (1.0–4.5 km) can be justified by the high quality of ERA5 data, computational efficiency considerations, and the successful experience of similar approaches in previous studies. Despite challenges associated with this large resolution jump, they can be managed through proper model configuration and rational sensitivity testing, for ensuring accurate and reliable high-resolution simulations (Warner et al., 1997; Giorgi and Mearns, 1999; Hersbach et al., 2020). In our research, we have a sufficient boundary buffer to prevent any boundary effects within the study area. Following the WRF user guide (National Center for Atmospheric Research, 2016a), 100 grid points are recommended. Accordingly, the eight domain sizes for the trial were generated using the same number of grid points. The recommended time step of six times grid resolution (in km) was applied (National Center for Atmospheric Research, 2016b). To adhere to the divisible feature of 3600 s, the time step values for case 1 and case 3 were adjusted from 27 s to 25 s and from 21 s to 20 s (in bold of Table 3), respectively. The specific settings of the eight domain tests for each rainfall event are as follows:

In the set of simulations listed in Table 3, different domain sizes are achieved by varying the grid resolution, in the context of similar computer resource (with this only changing slightly due to different time steps with changing grid resolution, based on the same number of grid points). Thus, differences between these simulations, for a given rainfall case, will reflect the impact of both changing the domain size and changing the grid resolution. Hence a number of additional sensitivity tests were carried out (see Section 3.5): varying grid resolution, but keeping domain size constant to isolate the influence of changing the grid resolution alone.

### 2.2.3. Model evaluations

This study chooses Kling-Gupta Efficiency (KGE), a widely used statistical indicator in hydrometeorology, for the WRF model evaluations. It considers the correlation and error in variation as well as the means of the simulation and the observation data respectively (Gupta et al., 2008) and integrates these into a single summary value (Kling et al., 2012; Reda et al., 2022). KGE can be expressed by Eq. (1):

**Table 4**  
Full information of eight rainfall events (reverse-chronological order, within newcastle boundary).

Event Number	The Simulated Time for Data Statistics	TCR (mm)	HMR (mm/h)	Rainfall Category and Rainfall Centre
reverse-chronological order	the last three days	observation: radar data	observation: radar data	References: BBC News Weather Reports (2020); BBC Weather Reports (2020); Met Office Synoptic Charts (2020); Met Office Weather (2020); Weather Online Historical Data (2023); Weather Com (2024); Weather Underground (2024)
1	19/08/2021–22/08/2021	~25	~3.5	Predominantly frontal rainfall; Concentrated in central and western Newcastle, with localised flooding in low-lying areas
2	25/08/2020–28/08/2020	~40	~8	Stratiform and convective rainfall; Eastern and central Newcastle experienced the heaviest rainfall
3	09/06/2020–12/06/2020	~30	~2.5	Primarily stratiform with some convective showers; Scattered across the region, with no significant concentration
4	11/06/2019–14/06/2019	~50	~9.5	Predominantly frontal rainfall; Concentrated in the urban areas of Newcastle
5	05/06/2017–08/06/2017	~70	~6	A mix of stratiform and convective rainfall; Southern Newcastle experienced the most intense rainfall
6	10/06/2016–13/06/2016	~10	~1	Stratiform rainfall; Evenly distributed across the region
7	04/06/2014–07/06/2014	~20	~4.5	Convective thunderstorms; Northern Newcastle and surrounding areas
8	15/07/2011–18/07/2011	~90	~7	Convective rainfall with severe thunderstorms; Western and central Newcastle was most affected

$$KGE = 1 - \sqrt{(r - 1)^2 + (\alpha - 1)^2 + (\beta - 1)^2} \tag{1}$$

where  $r$  is the correlation coefficient between the simulated data series and the observed data series,  $\alpha$  and  $\beta$  are the ratios of standard deviation and mean value between the two series, respectively (Gupta et al., 2009; Rummeler et al., 2019; Wang et al., 2022). Therefore, the evaluation results of the WRF model by KGE for rainfall simulation are more comprehensive compared to some common and simple statistical indicators, and the optimal performance is achieved when  $KGE = 1$ . The formula of the derived indicator for evaluating sensitivity analysis cases will be specified in Section 3.5.

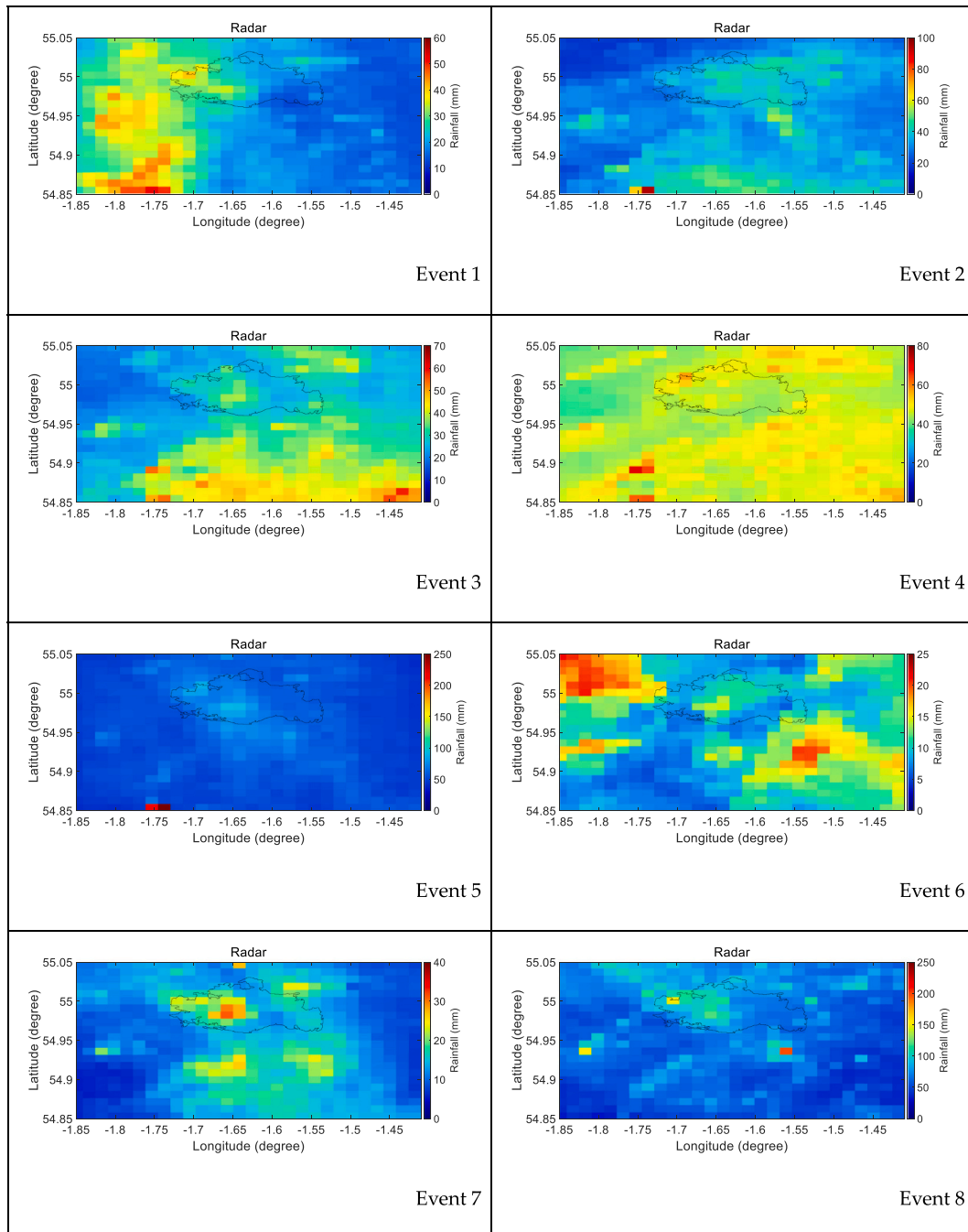
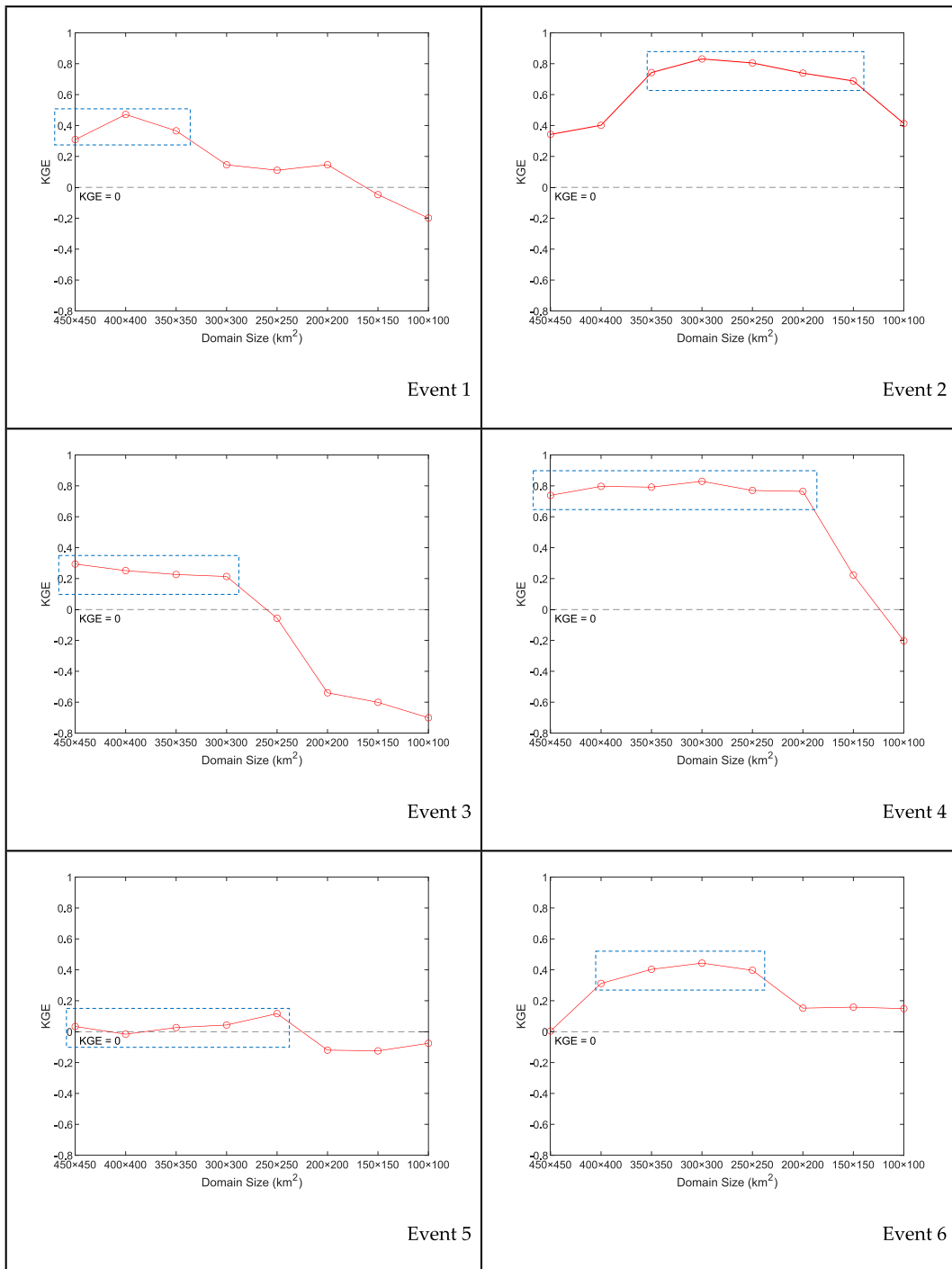


Fig. 2. Radar spatial distributions (showing the part of assigned radar area) of the accumulated precipitation (mm) over the last three days for the eight rainfall events.



**Fig. 3.** KGE line charts for the eight rainfall events. KGE is calculated using the hourly timeseries of rainfall, within the Newcastle Boundary for the last three days of each event. The KGE = 0 lines are shown in each subpanel. Clusters of similar datapoints with relatively high KGE values are framed in blue dashed boxes, based on a nearest-neighbour approach described in Section 3.3.

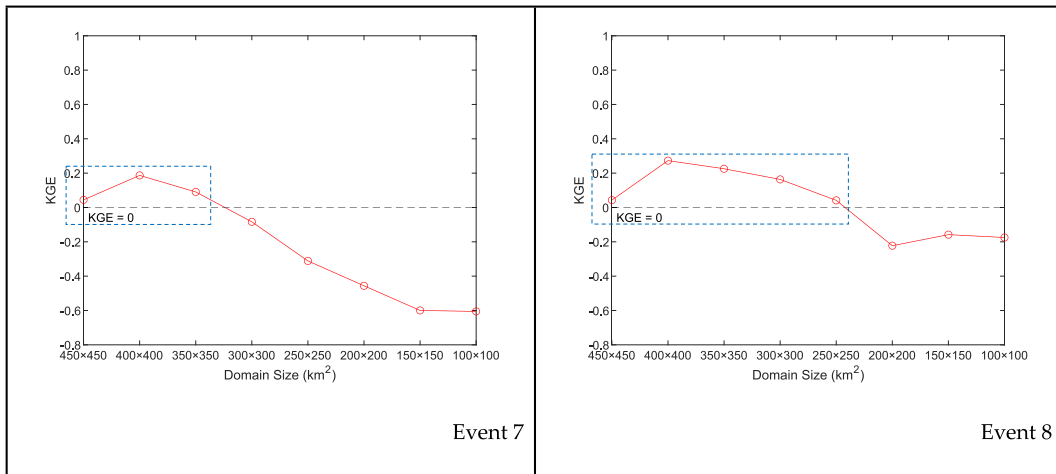


Fig. 3. (continued).

### 3. Results

#### 3.1. Overview of selected rainfall characteristics and observed radar maps

Generally, rainfall in winter is dominated by longer duration large-scale events, whilst in summer, there are more short duration intense events. Here, we only consider summer rainfall events which are expected to particularly benefit from the convection-permitting resolutions. In Table 4, the specific simulation time, detailed rainfall values and key rainfall characteristics for the eight rainfall events are listed, which is in a reverse-chronological order according to the occurrence time of rainfall. According to observations (time and date, 2021), the rainfall duration for all the selected events spans three days.

The radar maps of each rainfall event (resolution = 1 km) are shown in Fig. 2. Their rainfall intensities are listed in Table 4.

Looking in detail at Fig. 2, event 2, event 5 and event 8 have isolated pixels with exceptionally high rainfall occurring within the wider region surrounding Newcastle. To exclude spurious values, the radar hourly precipitation of each event was checked, ditto for WRF hourly precipitation. This did not show any evidence of spurious rainfall values impacting the results. We note for the following analysis of KGE, only the grid cells within the Newcastle boundary (marked by the black line in Fig. 2) are included.

#### 3.2. KGE-based evaluation of WRF simulations across rainfall events and domain sizes

KGE values for the 64 domain tests (8 rainfall events  $\times$  8 domain sizes, see Table 3 for detailed settings) are shown in Fig. 3.

In general, the eight rainfall events display a downward trend on KGE values with decreasing domain sizes and increasing grid resolutions. When domain size is smaller than  $150 \times 150 \text{ km}^2$ , nearly all the simulated cases for all the rainfall events perform rather poorly, despite having finer grid resolution. All the cases of event 2 and event 6 hold KGE values over 0, indicating that the overall simulation on domain size of these two rainfall events is not so bad. However, the remaining rainfall events include some KGE values less than 0 (event 1 cases: domain size  $\leq 150 \times 150 \text{ km}^2$ ; event 3 cases: domain size  $\leq 250 \times 250 \text{ km}^2$ ; event 4 case: domain size =  $100 \times 100 \text{ km}^2$ ; event 5 cases: domain size =  $400 \times 400 \text{ km}^2$  and domain size  $\leq 200 \times 200 \text{ km}^2$ ; event 7 cases: domain size  $\leq 300 \times 300 \text{ km}^2$ ; event 8 cases: domain size  $\leq 200 \times 200 \text{ km}^2$ ). What is more, there is not a clear relationship between performance and domain size for event 5. Event 4 has the most stable KGE values across the larger domain sizes (excluding  $150 \times 150 \text{ km}^2$  and  $100 \times 100 \text{ km}^2$ ). In addition, the majority of KGE values for the eight domain sizes of event 2 and event 4 reflect their better performance in rainfall simulation.

To explain the special pixels (very high observed values compared to the WRF simulated results) in Fig. 2, possible reasons include weaker constraints from the large-scale conditions imposed at the lateral boundary (for event 2) and rainfall misalignment in the WRF model (i.e., does not occur over Newcastle city) (for event 8). As shown in the subplot of Fig. 3, event 5 generally gets the lowest KGE scores among the eight rainfall events. One contributing factor to this poor performance is that the spatial distribution of rainfall in WRF differs substantially from that in radar (e.g., more localised showers as opposed to more uniform rain).

#### 3.3. The acceptable SDS ranges for varied rainfall events

The acceptable SDS ranges for the eight rainfall events are determined by the cluster analysis on the KGE values. Cluster analysis has various algorithms to classify a set of objects in such a way that objects in the same cluster are more similar to each other than to those in other clusters (Everitt et al., 2011). The concept of a “cluster” cannot be precisely defined, which partly explains the existence of numerous clustering algorithms, such as connectivity models, centroid models, graph-based models, and many more (Estivill-Castro, 2002). The cluster analysis algorithm adopted in this study is based on  $k$ -nearest neighbours algorithm where KGE deviations from the

maximum are used to partition the datapoints into two clusters: the nearest-maximum cluster and the distant-maximum cluster. The acceptable SDS ranges are selected from the nearest-maximum cluster (as indicated by the blue dashed boxes in Fig. 3) in which their KGE values are relatively high in contrast to those in the distant-maximum cluster. The border between these two clusters is visually judged instead of a fixed value due to diverse KGE distributions in different events. Further studies are needed to find a more objective and precise cluster border, although this would be a challenging task.

Based on the previous KGE line charts (see Fig. 3) at different domain sizes, Fig. 4 demonstrates the acceptable SDS ranges for each rainfall event in a reverse-chronological order, with orange points for upper limits and blue points for lower limits. The tested domain size range of the eight rainfall events is from  $150 \times 150 \text{ km}^2$  (minimum value) to  $450 \times 450 \text{ km}^2$  (maximum value), with a commonly accepted SDS enclosed by a green rectangle.

Although  $150 \times 150 \text{ km}^2$  domain size (the lower limit of event 2) falls within the acceptable SDS ranges, it occupies the smallest share (only one rainfall event) compared to the larger domain sizes ( $450 \times 450 \text{ km}^2$  for six events;  $400 \times 400 \text{ km}^2$  for seven events;  $350 \times 350 \text{ km}^2$  for eight events;  $300 \times 300 \text{ km}^2$  for six events;  $250 \times 250 \text{ km}^2$  for five events;  $200 \times 200 \text{ km}^2$  for two events). Furthermore,  $100 \times 100 \text{ km}^2$  should not be set as the domain size when simulating the eight summer rainfall events in Newcastle, as the acceptable SDS ranges for these events do not cover it at all.

According to Seth and Giorgi (1998), the location of lateral boundary should be sufficiently distant from the Region-Of-Interest (ROI) to avoid boundary artifacts. Accordingly, Jones et al. (1995) argued that a relatively large domain size for simulation is required, to ensure sufficient spin-up of small-scale features entering the model domain. Nevertheless, even with a smaller domain size, the initial and boundary conditions may be inconsistent due to possible error propagation from the lateral buffer zone to the ROI, resulting in influences on simulated results (Qian and Zubair, 2010). As a consequence, a sufficiently large domain size for the WRF model is needed (Maurya et al., 2018), which may explain the lower limit of acceptable domain size indicated from Fig. 4. We note however that too large a domain size may also be detrimental, with the high-resolution model no longer sufficiently constrained by the large-scale conditions prescribed at the lateral boundary.

### 3.4. A common optimal SDS

From Fig. 4 above,  $350 \times 350 \text{ km}^2$  (framed by a green rectangle in Fig. 4) is the common optimal SDS across the eight rainfall events. For the purpose of checking the reliability of the selected SDS, visualising each case of rainfall events is necessary. As previously mentioned, due to relatively large scale, event 4, with 50 mm TCR and 9.5 mm/h HMR, is the rainfall event with the best performance across domain size simulated by the WRF model. Relatively speaking, this event maintains good simulation stability throughout the eight domain sizes/grid resolutions across the eight rainfall events. Hence, taking it as an example for further study, the spatial distributions between observed data and simulated data for the eight domain sizes of this 2019 rainfall event are presented in Fig. 5.

Although 2019 rainfall is the best simulated event, some disagreement between observations and simulations is unavoidable just due to internal variability (since information on the observed state of the atmosphere is only fed into the model at the lateral boundary). By comparing the spatial distribution maps of radar data and the WRF data one by one, the domain sizes at  $150 \times 150 \text{ km}^2$  and  $100 \times 100 \text{ km}^2$  display the most significant differences, while the domain sizes at  $300 \times 300 \text{ km}^2$ ,  $400 \times 400 \text{ km}^2$  and  $350 \times 350 \text{ km}^2$  exhibit relative maximum similarity between observation and simulation. Moreover, as there are more simulation outliers

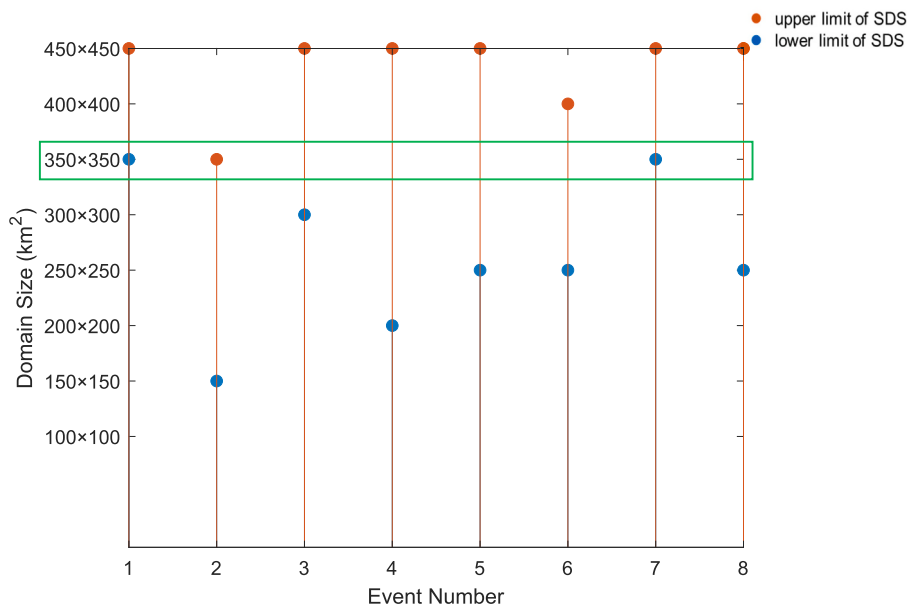
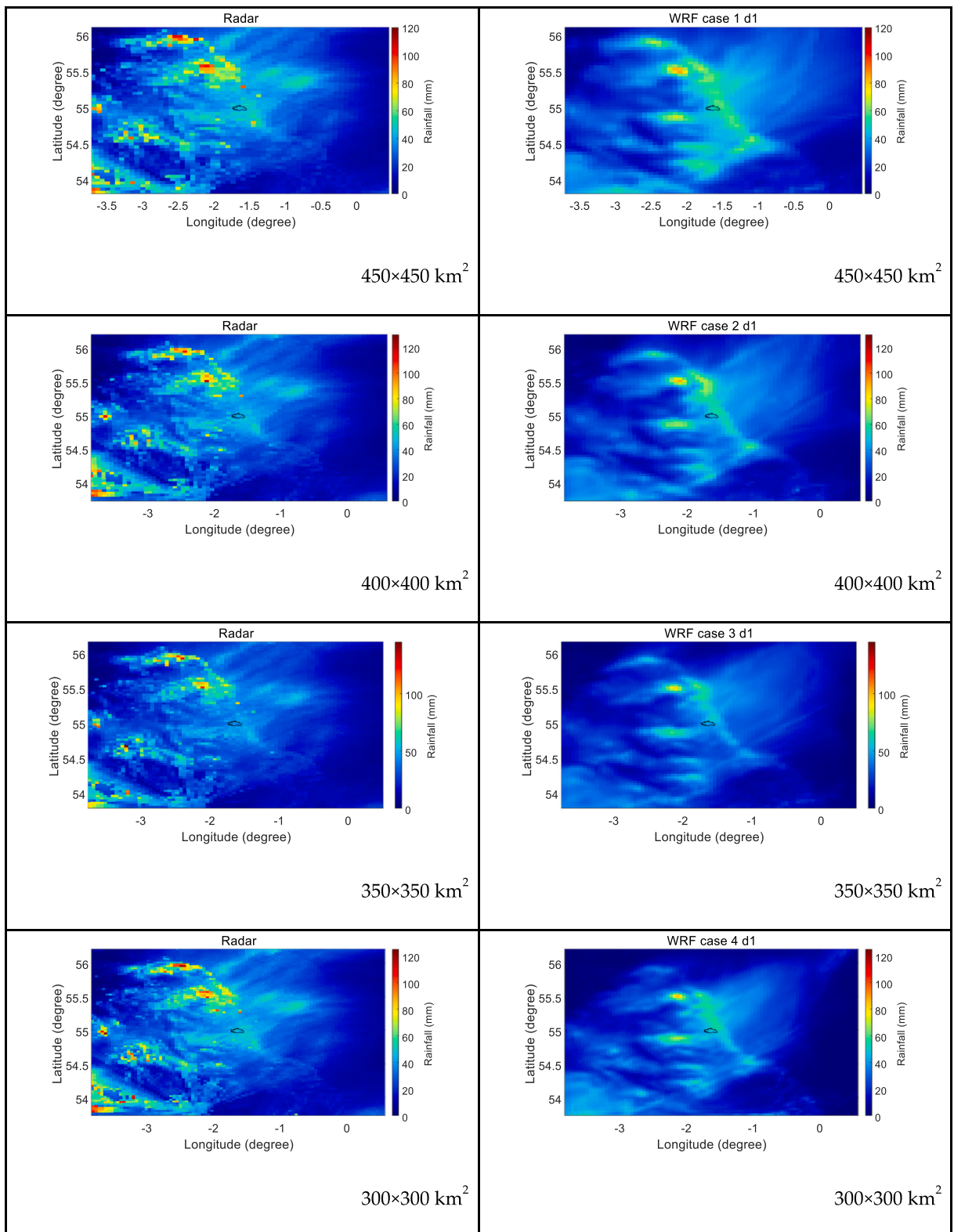


Fig. 4. The acceptable SDS ranges of Eight Rainfall Events (reverse-chronological order from near to far).



**Fig. 5.** Spatial distribution comparison between The WRF simulations with different model domain sizes (accompanying grid resolutions) and observations (constructed by regrided radar data) for the accumulated precipitation (mm) over the last three days of 2019 rainfall (event 4), shown in rainfall for the full extent of The WRF model domain.

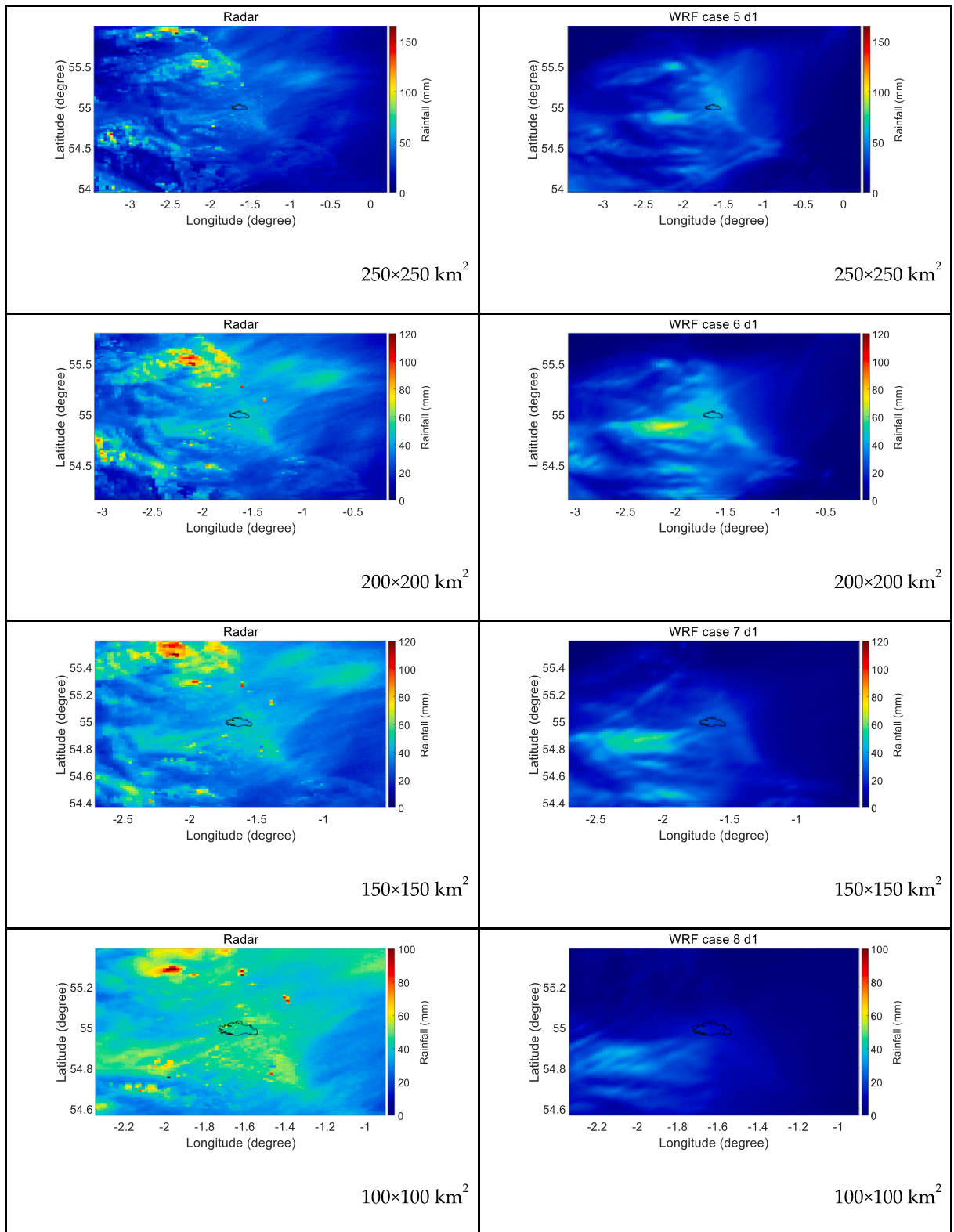


Fig. 5. (continued).

appearing in the spatial distribution maps of domain sizes at  $250 \times 250 \text{ km}^2$  and  $200 \times 200 \text{ km}^2$ , these two cases are inferior to the best three simulations (domain sizes at  $300 \times 300 \text{ km}^2$ ,  $400 \times 400 \text{ km}^2$  and  $350 \times 350 \text{ km}^2$ ) for this rainfall event. When domain size is  $450 \times 450 \text{ km}^2$ , the simulation result significantly overestimates the observed values, which may be explained by the coarser resolution of 4.5 km: as convectonal rainfall occurs over short periods and in localised regions, with coarse model resolution, it is difficult to capture its rainfall characteristics (McSweeney and Hausfather, 2018).

To establish a clearer order regarding the spatial distribution performance for 2019 rainfall event simulation, the sequential listing from better to worse on the basis of contrasting each pair of the domain sizes in Fig. 5 is: ① $300 \times 300 \text{ km}^2$ , ② $400 \times 400 \text{ km}^2$ , ③ $350 \times 350 \text{ km}^2$ , ④ $250 \times 250 \text{ km}^2$ , ⑤ $200 \times 200 \text{ km}^2$ , ⑥ $450 \times 450 \text{ km}^2$ , ⑦ $150 \times 150 \text{ km}^2$ , ⑧ $100 \times 100 \text{ km}^2$ . On the one hand, the performance ordering of domain size based on spatial distribution and KGE ( $300 \times 300 \text{ km}^2$ : 0.83;  $400 \times 400 \text{ km}^2$ : 0.80;  $350 \times 350 \text{ km}^2$ : 0.79;  $250 \times 250 \text{ km}^2$ : 0.77;  $200 \times 200 \text{ km}^2$ : 0.76;  $450 \times 450 \text{ km}^2$ : 0.74;  $150 \times 150 \text{ km}^2$ : 0.22;  $100 \times 100 \text{ km}^2$ : -0.20) remains consistent. On the other hand,  $350 \times 350 \text{ km}^2$  is in the third place where it is able to be the SDS for this rainfall event.  $450 \times 450 \text{ km}^2$ ,  $150 \times 150 \text{ km}^2$  and  $100 \times 100 \text{ km}^2$  are placed at the last three positions, reaffirming that both too large and too small domain sizes are unsuitable for the rainfall simulation in Newcastle.

### 3.5. Sensitivity analysis: The possible interference of grid resolution on the WRF simulation

There are two ways to adjust domain size: keeping grid resolution constant while varying the number of grid points or varying grid resolution but keeping the number of grid points constant. The latter (the results in Section 3.3 and Section 3.4) corresponds to constant computational cost, while the former results in a considerably increased cost for large domain sizes, especially at high grid resolution. On the other hand, high grid resolution for a given domain size contributes to improving the understanding of rainfall patterns in urban studies. The above results vary domain size by changing grid resolution, and hence it is difficult to disentangle extent to which improved performance is due to domain or resolution. We now explore the extent to which grid resolution differences (rather than domain size per se) may be an important contributing factor to the simulation accuracy by carrying out sensitivity tests (varying grid resolutions and the number of grid points & keeping the domain size fixed) (see Table 5). This approach becomes increasingly computationally expensive for finer grid resolutions.

To conduct the sensitivity analysis experiment, Table 5 shows specific values on time steps and three key elements: domain size, grid resolutions and grid points. As mentioned before, the first day of the eight rainfall events is designed as spin-up time and time step is determined by sixfold grid resolution. Thereinto, the bolds in Table 5 are the same meaning with them in Table 3. The common optimal SDS identified above as  $350 \times 350 \text{ km}^2$ , which is appropriate for each rainfall event, is used. In addition to the original configuration for grid resolution (3.5 km) and grid points (100), by adjusting the grid resolution up and down (with the corresponding grid points), the other seven combinations are: 4.5 km and 77, 4 km and 87, 3 km and 116, 2.5 km and 140, 2 km and 175, 1.5 km and 233, 1 km and 350, respectively.

To check the WRF simulation performance for each test of each rainfall event in this sensitivity analysis and compare the impacts of domain size and grid resolution on the simulated results at the same time, a relevant indicator deriving from KGE is introduced, referring to Eq. (2):

$$\Delta KGE = KGE - KGE_{3.5} \quad (2)$$

where  $\Delta KGE$  represents the distance between the KGE and the KGE at 3.5 km grid resolution ( $KGE_{3.5}$ ) simulated by the WRF model. On the one hand,  $350 \times 350 \text{ km}^2$  is the common optimal SDS for all the rainfall events with 3.5 km grid resolution and 100 grid point. On the other hand, such collocation is the original configuration for carrying out sensitivity analysis. Thus, this case plays a link role on general simulations and sensitive experiments, with all the  $KGE_{3.5}$  values set as the benchmark.

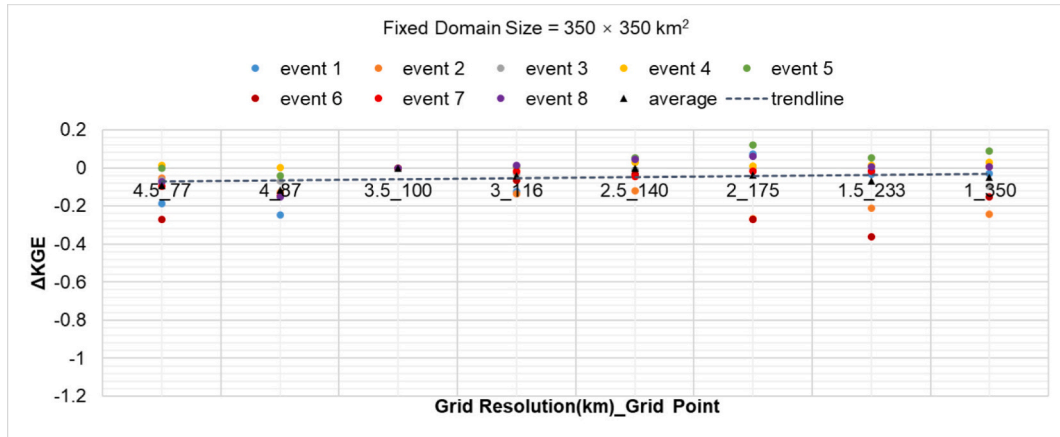
Fig. 6(a) displays all the difference values between KGE and  $KGE_{3.5}$  in the form of  $\Delta KGE$ , including eight resolution tests of each rainfall event. The average  $\Delta KGE$  values of the eight rainfall events at eight different grid resolution (from coarse to fine) and grid point combinations are presented in Fig. 6(a) as well: -0.092, -0.12, 0.00, -0.043, -0.0036, -0.036, -0.070, -0.048. Accordingly, the  $\Delta KGE$  values of each rainfall event, both for eight domain tests (different grid resolution but fixed grid point) and their each averages (-0.13, -0.024, 0.00, -0.036, -0.12, -0.30, -0.42, -0.53), are shown in Fig. 6(b).

Integrating all the data points together (triangle for average, dot for individual) for consideration, the data distribution displayed in Fig. 6(a) gathers together more than those in Fig. 6(b). As for the span of minimum  $\Delta KGE$  and maximum  $\Delta KGE$ , sensitivity analysis

**Table 5**  
Sensitivity analysis configurations (within Newcastle Boundary).

Domain Size ( $\text{km}^2$ )	Grid Resolution (km)	Grid Point	Time Step (s)	
350 × 350	case1	4.5	77	25
	case2	4	87	24
	case3	3.5	100	20
	case4	3	116	18
	case5	2.5	140	15
	case6	2	175	12
	case7	1.5	233	9
	case8	1	350	6

(a)



(b)

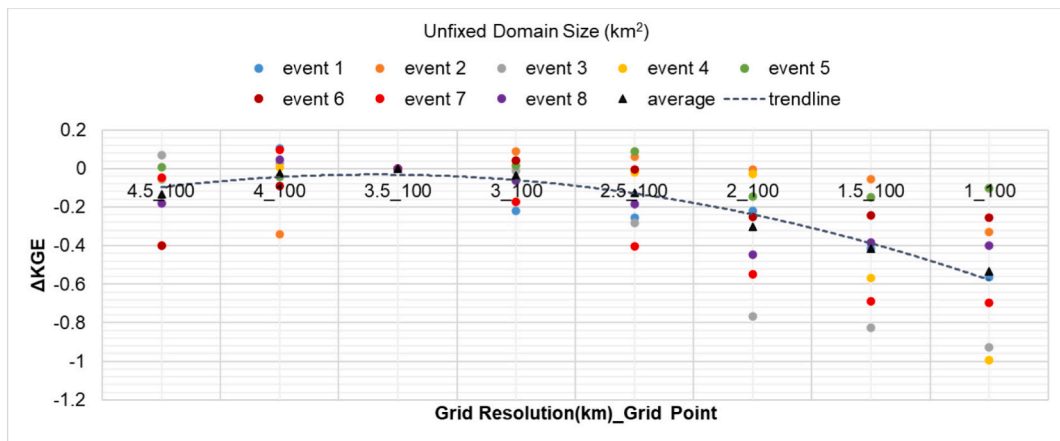


**Fig. 6.** Relative influence of changing grid resolution (at fixed domain size) versus varying domain size (at fixed grid point number). Fitted Line Plot for  $\Delta KGE$ : (a) eight resolution tests of the eight rainfall events for sensitivity analysis; (b) eight domain tests of each rainfall event.

cases ( $\sim 0.48$ : from  $-0.36$  to  $0.12$ ) are far less than original configuration cases ( $\sim 1.1$ : from  $-1.0$  to  $0.11$ ), signifying that the simulation results among the former are more similar. This indicates that the results presented previously, do not simply reflect changing grid resolution, with domain size a key determining factor at performance. Hence, setting domain size by varying grid resolution is justifiable because of the minor interference, providing remain in convection-permitting regime ( $< 5$  km).

Under the fixed domain size ( $350 \times 350 \text{ km}^2$ ), as the grid resolution increases, providing within convection-permitting regime, the linear trendline of average  $\Delta KGE$  generally demonstrates upward tendency but the overall slope is getting smaller and smaller, suggesting that the higher grid resolution can slightly improve the WRF simulation performance, but with such influence, getting less and

**Table 6**

The list for eight rainfall events (TCR order and HMR order).

Event Number	The Acceptable SDS Ranges	Event Number	The Acceptable SDS Ranges
TCR order	lower limit–upper limit	HMR order	lower limit–upper limit
8	$250 \times 250 \text{ km}^2$ – $450 \times 450 \text{ km}^2$	4	$200 \times 200 \text{ km}^2$ – $450 \times 450 \text{ km}^2$
5	$250 \times 250 \text{ km}^2$ – $450 \times 450 \text{ km}^2$	2	$150 \times 150 \text{ km}^2$ – $350 \times 350 \text{ km}^2$
4	$200 \times 200 \text{ km}^2$ – $450 \times 450 \text{ km}^2$	8	$250 \times 250 \text{ km}^2$ – $450 \times 450 \text{ km}^2$
2	$150 \times 150 \text{ km}^2$ – $350 \times 350 \text{ km}^2$	5	$250 \times 250 \text{ km}^2$ – $450 \times 450 \text{ km}^2$
3	$300 \times 300 \text{ km}^2$ – $450 \times 450 \text{ km}^2$	7	$350 \times 350 \text{ km}^2$ – $450 \times 450 \text{ km}^2$
1	$350 \times 350 \text{ km}^2$ – $450 \times 450 \text{ km}^2$	1	$350 \times 350 \text{ km}^2$ – $450 \times 450 \text{ km}^2$
7	$350 \times 350 \text{ km}^2$ – $450 \times 450 \text{ km}^2$	3	$300 \times 300 \text{ km}^2$ – $450 \times 450 \text{ km}^2$
6	$250 \times 250 \text{ km}^2$ – $400 \times 400 \text{ km}^2$	6	$250 \times 250 \text{ km}^2$ – $400 \times 400 \text{ km}^2$

less with finer and finer grid resolution. In Fig. 6(b), with the diminishing domain size, the polynomial trendline of average  $\Delta KGE$  overall presents downward tendency, along with the general slope becoming bigger and bigger, meaning that the smaller domain size may weaken the WRF simulation performance to a greater extent.

#### 4. Discussion

Here we discuss the extent to which we can explain the optimal SDS variation across the eight precipitation events based on the varying precipitation characteristics of each event. In particular, we explore the relationship of the acceptable SDS range with rainfall amount (including TCR and HMR) and rainfall spatial coverage. Additionally, we provide a comparative analysis on SDS for urban rainfall simulations and discuss the limitations of our study.

##### 4.1. The regular pattern between rainfall amount and SDS

The left side of Table 6 lists eight rainfall events in the order from large to small TCR based on radar data (for specific values, see Table 4), reflecting rainfall amount diversity (from  $\sim 10$  mm to  $\sim 90$  mm) from the perspective of accumulated value. Similarly, the order from large to small on the observed value of HMR (ditto, see Table 4) is presented in the right side of Table 6, displaying a wide span (from  $\sim 1$  mm/h to  $\sim 9.5$  mm/h) on the max rainfall rate. Moreover, the acceptable SDS ranges (determined by the KGE performance of eight rainfall events in Fig. 3), from the lower limit to the upper limit of domain size, are listed in Table 6, following the orders of TCR and HMR (visualization: see Fig. 7 and Fig. 8, respectively).

A similar relationship is observed between acceptable SDS range and rainfall intensity, whether measured using TCR or HMR (Fig. 7 and Fig. 8). Namely as rainfall amounts decrease, there is a tendency for a narrower acceptable SDS range (with higher lower limits), centred on larger domain sizes, while the smaller domain sizes are only suitable for heavier events.

##### 4.2. The regular pattern between rainfall amount and rainfall spatial coverage in term of SDS

Next, we explore the relationship between rainfall amount and rainfall spatial coverage with SDS. Table 7 ranks the rainfall spatial coverages of the eight rainfall events on the basis of the spatial distribution maps in Fig. 2. The event sequence of precipitation spatial coverages (mainly considering the observations within Newcastle boundary) from large to small and the corresponding acceptable SDS ranges for each event are listed:

In accordance with the sequence in Table 7, Fig. 9 plots the eight rainfall events in the order of rainfall spatial coverage from large to small and displays their corresponding acceptable SDS ranges.

The ordering of rainfall events by spatial coverage is slightly different than the ordering by rainfall amount (both TCR and HMR). Among them, event 8, which is classified as one of the heavier rainfall events, has the smaller spatial coverage, whilst event 3, classified as one of the lighter rainfall events, is in the larger spatial coverage category, however there is reasonable correspondence between rainfall amount and event spatial size, with the heaviest events also tending to have larger spatial coverage. Consequently, there is a similar tendency for smaller sized events to favour larger domain sizes, with the smallest domain sizes only suitable for the spatially

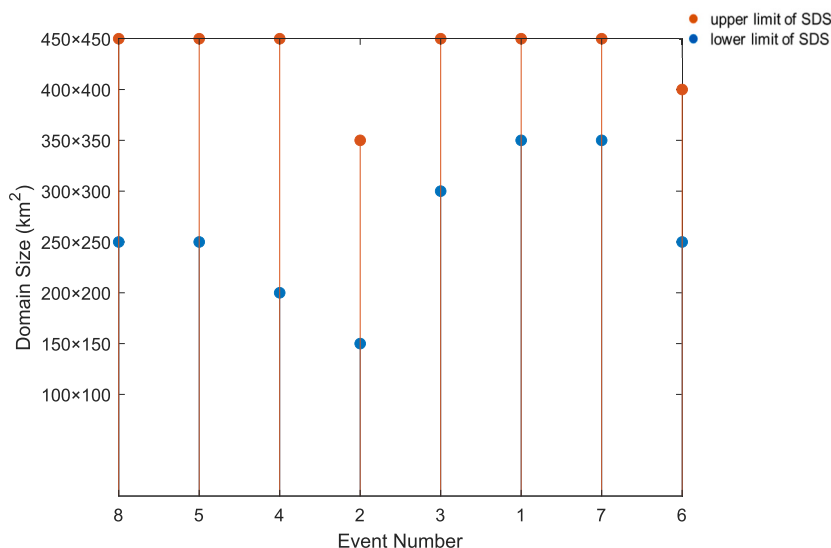


Fig. 7. The acceptable SDS ranges of eight rainfall events (TCR order from heavy to light).

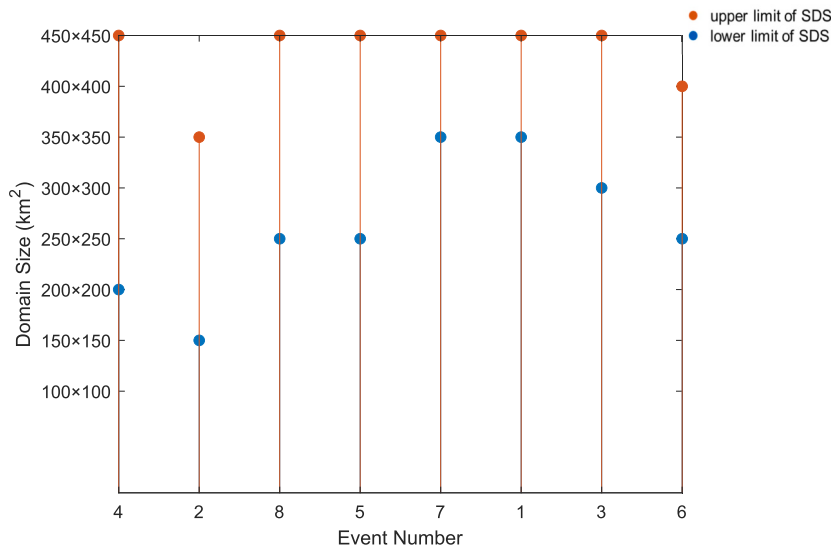


Fig. 8. The acceptable SDS ranges of eight rainfall events (HMR order from heavy to light).

Table 7

The list for eight rainfall events (rainfall spatial coverage order, focusing on the area within Newcastle Boundary).

Event Number	Rainfall Spatial Coverage	The Acceptable SDS Ranges
Rainfall spatial coverage order	Observation: radar data	Lower limit–upper limit
4		200 × 200 km <sup>2</sup> –450 × 450 km <sup>2</sup>
2		150 × 150 km <sup>2</sup> –350 × 350 km <sup>2</sup>
5	Large	250 × 250 km <sup>2</sup> –450 × 450 km <sup>2</sup>
3		300 × 300 km <sup>2</sup> –450 × 450 km <sup>2</sup>
7	↓	350 × 350 km <sup>2</sup> –450 × 450 km <sup>2</sup>
8		250 × 250 km <sup>2</sup> –450 × 450 km <sup>2</sup>
6	Small	250 × 250 km <sup>2</sup> –400 × 400 km <sup>2</sup>
1		350 × 350 km <sup>2</sup> –450 × 450 km <sup>2</sup>

more extensive events, although the relationship is less clear than with rainfall amount. This behaviour may be explained by the fact that the smaller-scale events need more time to spin up on entering the domain than larger-scale events that are already well represented in the driving model.

#### 4.3. Comparative analysis: SDS for urban rainfall simulations

By comparing our results on the SDS for simulating urban rainfall using the WRF model with those from other cases, we compare this work with previous studies. We show that the domain sizes smaller than 150 × 150 km<sup>2</sup> are insufficient to reliably simulate summer rainfall events over Newcastle. Yu et al. (2022) investigated the impacts of the WRF model domain size on Meiyu forecasts. Their research revealed that an appropriately enlarged domain size better captured weather systems and associated precipitation, leading to significant improvements in forecast accuracy. This conclusion is consistent with the finding of us. We identify a common optimal SDS of 350 × 350 km<sup>2</sup> across eight rainfall events. Chu et al. (2018) highlighted that rainfall simulations were highly sensitive to domain sizes, with larger domain sizes improving the accuracy of rainfall intensity and spatial correlation. However, overly large ones might introduce computational inefficiencies without performance gains. Both studies agree that excessively large domain sizes (e.g., 450 × 450 km<sup>2</sup>) are not ideal. We discover that lighter and spatially more confined rainfall events benefit from larger domain sizes. In contrast, the heaviest and spatially more extensive rainfall events can still be reasonably represented even with the smallest domain sizes. Opio et al. (2020) conducted WRF simulations of extreme rainfall over Uganda and assessed sensitivity to parameterisation, grid resolution and domain size. They emphasised the importance of larger domain sizes to capture lighter and more localised rainfall events, aligning with one of our results.

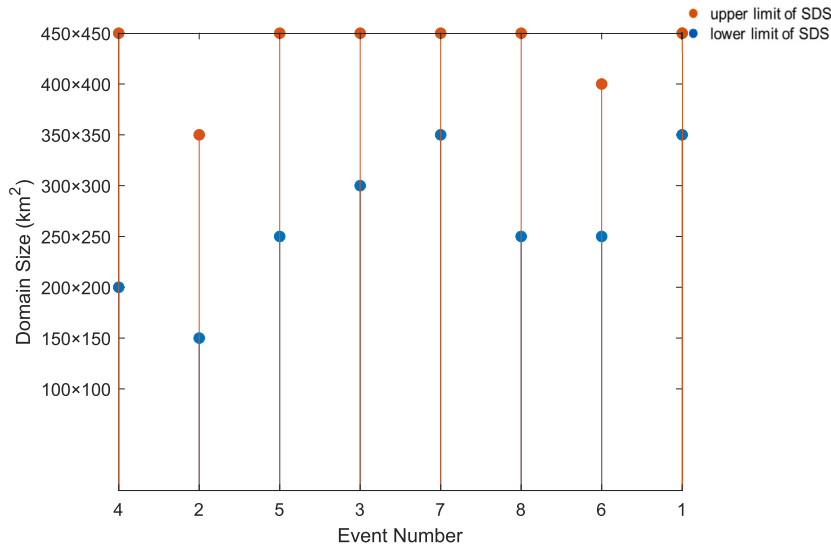


Fig. 9. The acceptable SDS ranges of eight rainfall events (rainfall spatial coverage order from large to small).

#### 4.4. Limitations

Limitations of this study relate to sample size, general applicability, model utilisation and scheme configuration. To assess the robustness of the findings, more events especially for winter rainfall are needed: the rainfall in UK is characterised by frequent and intense rainfall in summer but short duration, as opposed to winter rainfall which is predominately from large-scale events. Based on results here (events with larger spatial size are suitable for smaller domain size), smaller domain size ( $100 \times 100 \text{ km}^2$ ) may be suitable for winter rainfall events. Also, more cities should be simulated (Du et al., 2023). Similarly, here only the single domain case of the WRF model has been explored, so the analysis for nested model runs will be the next step. Last but not least, on account of the specificity in urban hydrometeorological studies, modifying the related settings of the WRF-urban modelling is a great help to produce a more robust rainfall simulation responding to the series of urban environmental issues resulting from urbanisation impact (National Center for Atmospheric Research, 2023) on which Zhang et al. (2018) conducted a case study by comparing the differences of two sets (the WRF model coupled with the Noah land surface model and the multi-layer Building Energy Model (BEM) as well as using croplands in spite of urban land-use types and retaining other settings). As a consequence, identifying how the optimal domain size and model configuration varies from city to city will be the subject of future work (Du et al., 2022).

#### 5. Conclusions

This study examines how well WRF model simulates urban rainfall and aims to identify the optimal model configuration (domain size) and relevant change rule for given computational resource, including: (1) The acceptable SDS ranges for eight rainfall events; (2) A common optimal SDS; (3) The relationship between rainfall characteristics, including rainfall amount and rainfall spatial coverage, and the acceptable SDS ranges. Eight Newcastle rainfall events occurring during summer over the past 13 years were explored. Key conclusions are:

- 1 When simulating with the WRF model for the eight summer rainfall events, the simulation performance is notably poor when domain size is less than  $150 \times 150 \text{ km}^2$ . Thus, using the grid resolution of 1 km and the recommended 100 grid points, domain size ( $100 \times 100 \text{ km}^2$ ) is found to be too small for satisfactory simulation of rainfall.
- 2 By integrating all domain tests (64 in total),  $350 \times 350 \text{ km}^2$  emerges as the common optimal SDS that is covered within the acceptable SDS ranges for the eight rainfall events. The visual analysis of the events confirms that the domain size for the rainfall simulation here should not be too large ( $450 \times 450 \text{ km}^2$ ) either.

Additional sensitivity experiments show that while varying grid resolution (within the convection-permitting regime) at fixed domain size ( $350 \times 350 \text{ km}^2$ ) does affect model performance, the impact is generally less significant compared to the changes in domain size. This indicates that domain size plays a more critical role than grid resolution in influencing WRF modelling performance for these rainfall events.

- 3 In terms of the rainfall characteristics, there is a tendency for lighter smaller sized events to favour larger domain sizes, with the smallest domain sizes only suitable for the heaviest spatially more extensive events. This is consistent with the need for greater spin up of small-scale features entering the domain.

Although the results presented here are for Newcastle city, we anticipate that sensitivity to domain size (specifically time for rainfall events to spin up on entering the domain and the level of constraint imposed by the lateral boundary conditions) will apply in other cities and we invite the community to consider this when choosing optimal simulation set-ups for urban rainfall modelling. Looking ahead, the study plans to extend its methods to other cities and additional events, including winter scenarios where smaller domain sizes might suffice due to the generally larger-scale nature of winter rainfall. It also tends to assess whether optimal model setup (the WRF nesting simulation and the WRF-Urban Setting) follows similar principles.

### Author statement

We declare that this manuscript is original, has not been published before and is not currently being considered for publication elsewhere.

We confirm that the manuscript has been read and approved by all named authors and that there are no other persons who satisfied the criteria for authorship but are not listed. We further confirm that the order of authors listed in the manuscript has been approved by all of us.

We understand that the corresponding author is the sole contact for the editorial process. She is responsible for communicating with the other authors about progress, submissions of revisions and final approval of proofs.

### Funding

Sichan Du is funded by the joint PhD scholarships (202009110149) from the China Scholarship Council (CSC) and the University of Bristol (UoB). Elizabeth J. Kendon is grateful for funding under the Hadley Centre Climate Programme funded by the UK Department for Science Innovation and Technology (DSIT) (GA01101).

### CRediT authorship contribution statement

**Sichan Du:** Writing – original draft, Visualization, Validation, Software, Methodology, Investigation, Formal analysis, Data curation, Conceptualization. **Lu Zhuo:** Writing – review & editing, Visualization, Supervision, Methodology, Data curation, Conceptualization. **Elizabeth J. Kendon:** Writing – review & editing, Supervision, Methodology, Conceptualization. **Dawei Han:** Writing – review & editing, Supervision, Methodology, Conceptualization.

### Declaration of competing interest

The authors declare the following financial interests/personal relationships which may be considered as potential competing interests: Sichan Du reports financial support was provided by China Scholarship Council. Elizabeth J. Kendon reports financial support was provided by DSIT. If there are other authors, they declare that they have no known competing financial interests or personal relationships that could have appeared to influence the work reported in this paper.

### Acknowledgments

This work was carried out using the computational facilities of the Advanced Computing Research Centre, University of Bristol - <http://www.bristol.ac.uk/acrc/>.

### Data availability

Data will be made available on request.

### References

- BBC News Weather Reports, 2020. BBC NEWS. British Broadcasting Corporation. <https://www.bbc.co.uk/news>. accessed on 19 August 2024.
- BBC Weather Reports, 2020. BBC WEATHER. British Broadcasting Corporation. <https://www.bbc.co.uk/weather>. accessed on 19 August 2024.
- Bhaskaran, B., Ramachandran, A., Jones, R., Moufouma-Okia, W.I.S.S.N., 2012. Regional climate model applications on sub-regional scales over the Indian monsoon region: the role of domain size on downscaling uncertainty. *J. Geophys. Res. Atmos.* 117 (D10).
- bluegreencities, 2013. WP5. Newcastle - the Demonstration City. The University of Nottingham. <http://www.bluegreencities.ac.uk/research/newcastle-as-demonstration-city.aspx> (accessed on 4 June 2023).
- Bonekamp, P.N.J., Collier, E., Immerzeel, W.W., 2018. The impact of spatial resolution, land use, and spinup time on resolving spatial precipitation patterns in the Himalayas. *J. Hydrometeorol.* 19 (10), 1565–1581.
- Cheng, W.Y., Liu, Y., Liu, Y., Zhang, Y., Mahoney, W.P., Warner, T.T., 2013. The impact of model physics on numerical wind forecasts. *Renew. Energy* 55, 347–356.
- Chu, Q., Xu, Z., Chen, Y., Han, D., 2018. Evaluation of the ability of the Weather research and forecasting model to reproduce a sub-daily extreme rainfall event in Beijing, China using different domain configurations and spin-up times. *Hydrol. Earth Syst. Sci.* 22 (6), 3391–3407.
- Cui, C., Bao, Y., Yuan, C., Li, Z., Zong, C., 2019. Comparison of the performances between the WRF and WRF-LES models in radiation fog—a case study. *Atmos. Res.* 226, 76–86.
- Dash, S.K., Pattanayak, K.C., Panda, S.K., Vaddi, D., Mangain, A., 2015. Impact of domain size on the simulation of Indian summer monsoon in RegCM4 using mixed convection scheme and driven by HadGEM2: impact of domain size on ISM simulations. *Clim. Dyn.* 44, 961–975.
- Dee, D.P., Uppala, S.M., Simmons, A.J., Berrisford, P., Poli, P., Kobayashi, S., Andrae, U., Balmaseda, M.A., Balsamo, G., Bauer, D.P., Bechtold, P., 2011. The ERA-interim reanalysis: configuration and performance of the data assimilation system. *Q. J. R. Meteorol. Soc.* 137 (656), 553–597.

- Deng, A., Stauffer, D.R., 2006. On improving 4-km mesoscale model simulations. *J. Appl. Meteorol. Climatol.* 45 (3), 361–381.
- Du, S., Zhuo, L., Kendon, E.J., Han, D., Liu, Y., Wang, J., Wang, Q., 2022, May. WRF simulations on the impacts and responses of extreme weather events: from the perspectives of climate change and urbanisation over UK cities. In: EGU General Assembly Conference Abstracts (pp. EGU22-5144).
- Du, S., Zhuo, L., Kendon, E.J., Han, D., 2023. Exploring Domain Size for WRF High-Resolution Urban Rainfall Simulation, vols. EGU23-8950. Copernicus Meetings.
- Duan, W., Hanasaki, N., Shioyama, H., Chen, Y., Zou, S., Nover, D., Zhou, B., Wang, Y., 2019. Evaluation and future projection of Chinese precipitation extremes using large ensemble high-resolution climate simulations. *J. Clim.* 32 (8), 2169–2183.
- Dudhia, J., 1989. Numerical study of convection observed during the winter monsoon experiment using a mesoscale two-dimensional model. *J. Atmos. Sci.* 46 (20), 3077–3107.
- Estivill-Castro, V., 2002. Why so many clustering algorithms: a position paper. *ACM SIGKDD Explor. Newslett.* 4 (1), 65–75.
- Everitt, B., Landau, S.L., Leese, M., 2011. *Cluster Analysis*.
- Feng, Z., Leung, L.R., Houze Jr., R.A., Hagos, S., Hardin, J., Yang, Q., Han, B., Fan, J., 2018. Structure and evolution of mesoscale convective systems: sensitivity to cloud microphysics in convection-permitting simulations over the United States. *J. Adv. Model. Earth Syst.* 10 (7), 1470–1494.
- Fosser, G., Kendon, E., Chan, S., Lock, A., Roberts, N., Bush, M., 2020. Optimal configuration and resolution for the first convection-permitting ensemble of climate projections over the United Kingdom. *Int. J. Climatol.* 40 (7), 3585–3606.
- Giorgi, F., Mearns, L.O., 1999. Introduction to special section: regional climate modeling revisited. *J. Geophys. Res. Atmos.* 104 (D6), 6335–6352.
- Google Earth Pro, 2022. Version 7.3, Google Inc. [software]. Retrieved 16 July 2023, from: [https://www.google.com/intl/en\\_uk/earth/about/versions/#earth-pro](https://www.google.com/intl/en_uk/earth/about/versions/#earth-pro).
- Goswami, P., Shivappa, H., Goud, S., 2012. Comparative analysis of the role of domain size, horizontal resolution and initial conditions in the simulation of tropical heavy rainfall events. *Meteorol. Appl.* 19 (2), 170–178.
- Gupta, H.V., Wagener, T., Liu, Y., 2008. Reconciling theory with observations: elements of a diagnostic approach to model evaluation. *Hydrol. Processes Int. J.* 22 (18), 3802–3813.
- Gupta, H.V., Kling, H., Yilmaz, K.K., Martinez, G.F., 2009. Decomposition of the mean squared error and NSE performance criteria: implications for improving hydrological modelling. *J. Hydrol.* 377 (1–2), 80–91.
- Hall, J., Solomatine, D., 2008. A framework for uncertainty analysis in flood risk management decisions. *Int. J. River Basin Manag.* 6 (2), 85–98.
- Harrison, D.L., Driscoll, S.J., Kitchen, M., 2000. Improving precipitation estimates from weather radar using quality control and correction techniques. *Meteorol. Appl.* 7 (2), 135–144.
- Herbach, H., Dee, D., 2016. ERA5 reanalysis is in production. *ECMWF Newslett.* No. 147 (ECMWF, Reading, United Kingdom, 7).
- Hersbach, H., Bell, B., Berrisford, P., Hirahara, S., Horányi, A., Muñoz-Sabater, J., Nicolas, J., Peubey, C., Radu, R., Schepers, D., Simmons, A., 2020. The ERA5 global reanalysis. *Q. J. R. Meteorol. Soc.* 146 (730), 1999–2049.
- Hewage, P., Trovati, M., Pereira, E., Behera, A., 2021. Deep learning-based effective fine-grained weather forecasting model. *Pattern. Anal. Applic.* 24 (1), 343–366.
- Hwang, S.O., Park, J., Kim, H.M., 2019. Effect of hydrometeor species on very-short-range simulations of precipitation using ERA5. *Atmos. Res.* 218, 245–256.
- Janić, Z.I., 2001. Nonsingular Implementation of the Mellor-Yamada Level 2.5 Scheme in the NCEP Meso Model.
- Janjić, Z.I., 1994. The step-mountain eta coordinate model: further developments of the convection, viscous sublayer, and turbulence closure schemes. *Mon. Weather Rev.* 122 (5), 927–945.
- Janjić, Z.I., 1996. The surface layer in the NCEP Eta model. In: Eleventh Conference on Numerical Weather Prediction, Norfolk, VA, 19–23 August 1996. Amer Meteor Soc, Boston, MA, pp. 354–355.
- Jin, Z., Ge, F., Chen, Q., Lin, Z., 2023. To what extent horizontal resolution improves the simulation of precipitation in CMIP6 HighResMIP models over Southwest China? *Front. Earth Sci.* 10, 1982.
- Jones, R.G., Murphy, J.M., Noguer, M., 1995. Simulation of climate change over Europe using a nested regional-climate model. I: assessment of control climate, including sensitivity to location of lateral boundaries. *Q. J. R. Meteorol. Soc.* 121 (526), 1413–1449.
- Jong, B.T., Delworth, T.L., Cooke, W.F., Tseng, K.C., Murakami, H., 2023. Increases in extreme precipitation over the Northeast United States using high-resolution climate model simulations. *npj Clim. Atmosph. Sci.* 6 (1), 18.
- Kendon, E., Short, C., Pope, J., Chan, S., Wilkinson, J., Tucker, S., Bett, P., Harris, G., 2021. Update to UKCP Local (2.2km) Projections. UK Met Office. [https://www.metoffice.gov.uk/pub/data/weather/uk/ukcp18/science-reports/ukcp18\\_local\\_update\\_report\\_2021.pdf](https://www.metoffice.gov.uk/pub/data/weather/uk/ukcp18/science-reports/ukcp18_local_update_report_2021.pdf) (accessed on 24 April 2024).
- Kharin, V.V., Zwiers, F.W., Zhang, X., Wehner, M., 2013. Changes in temperature and precipitation extremes in the CMIP5 ensemble. *Clim. Chang.* 119, 345–357.
- Kim, I.W., Oh, J., Woo, S., Kripalani, R.H., 2019. Evaluation of precipitation extremes over the Asian domain: observation and modelling studies. *Clim. Dyn.* 52, 1317–1342.
- Kling, H., Fuchs, M., Paulin, M., 2012. Runoff conditions in the upper Danube basin under an ensemble of climate change scenarios. *J. Hydrol.* 424, 264–277.
- Leduc, M., Laprise, R., 2009. Regional climate model sensitivity to domain size. *Clim. Dyn.* 32, 833–854.
- Liu, Z., Liu, Y., Wang, S., Yang, X., Wang, L., Baig, M.H.A., Chi, W., Wang, Z., 2018. Evaluation of spatial and temporal performances of ERA-interim precipitation and temperature in mainland China. *J. Clim.* 31 (11), 4347–4365.
- Liu, Y., Zhuo, L., Han, D., 2023. Developing spin-up time framework for WRF extreme precipitation simulations. *J. Hydrol.* 620, 129443.
- Mahoney, K., Alexander, M., Scott, J.D., Barsugli, J., 2013. High-resolution downscaled simulations of warm-season extreme precipitation events in the Colorado front range under past and future climates. *J. Clim.* 26 (21), 8671–8689.
- Manola, I., Steeneveld, G.J., Uijlenhoet, R., Holtslag, A.A., 2020. Analysis of urban rainfall from hourly to seasonal scales using high-resolution radar observations in the Netherlands. *Int. J. Climatol.* 40 (2), 822–840.
- Martilli, A., Clappier, A., Rotach, M.W., 2002. An urban surface exchange parameterisation for mesoscale models. *Bound.-Layer Meteorol.* 104 (2), 261–304.
- Maurya, R.K.S., Sinha, P., Mohanty, M.R., Mohanty, U.C., 2018. RegCM4 model sensitivity to horizontal resolution and domain size in simulating the Indian summer monsoon. *Atmos. Res.* 210, 15–33.
- McSweeney, R., Hausfather, Z., 2018. Q&A: How do Climate Models Work? Carbon Brief. <https://www.carbonbrief.org/qa-how-do-climate-models-work/>.
- Ménégou, M., Gallée, H., Jacobi, H.W., 2013. Precipitation and snow cover in the Himalaya: from reanalysis to regional climate simulations. *Hydrol. Earth Syst. Sci.* 17 (10), 3921–3936.
- Mesinger, F., 1993. Forecasting upper tropospheric turbulence within the framework of the Mellor-Yamada 2.5 closure. *Res. Activ. Atmos. Oceanic Mod.* 4–28.
- Met Office Synoptic Charts, 2020. Surface Pressure Charts. UK Met Office. <https://www.metoffice.gov.uk/weather/maps-and-charts/surface-pressure>. accessed on 19 August 2024.
- Met Office Weather, 2020. Find a Forecast. UK Met Office. <https://www.metoffice.gov.uk/>. accessed on 19 August 2024.
- Mitra, C., Shepherd, J.M., 2015. Urban precipitation: A global perspective. In: *The Routledge Handbook of Urbanization and Global Environmental Change*. Routledge, pp. 176–192.
- Mlawer, E.J., Taubman, S.J., Brown, P.D., Iacono, M.J., Clough, S.A., 1997. Radiative transfer for inhomogeneous atmospheres: RRTM, a validated correlated-k model for the longwave. *J. Geophys. Res. Atmos.* 102 (D14), 16663–16682.
- Monin, A.S., Obukhov, A.M., 1954. Basic laws of turbulent mixing in the surface layer of the atmosphere. *Contrib. Geophys. Inst. Acad. Sci. USSR* 151 (163), e187.
- Nacar, S., Kankal, M., Okkan, U., 2022. Evaluation of the suitability of NCEP/NCAR, ERA-Interim and ERA5 reanalysis data sets for statistical downscaling in the Eastern Black Sea Basin, Turkey. *Meteorol. Atmos. Phys.* 134 (2), 39.
- National Center for Atmospheric Research, 2004. WRF Model Users' Page. University Corporation for Atmospheric Research. <https://www2.mmm.ucar.edu/wrf/users/>. accessed on 22 November 2023.
- National Center for Atmospheric Research, 2016a. NAMELIST.WPS: Best Practices. University Corporation for Atmospheric Research. [https://www2.mmm.ucar.edu/wrf/users/namelist\\_best\\_prac\\_wps.html](https://www2.mmm.ucar.edu/wrf/users/namelist_best_prac_wps.html). accessed on 15 June 2023.
- National Center for Atmospheric Research, 2016b. NAMELIST.INPUT: Best Practices. University Corporation for Atmospheric Research. [https://www2.mmm.ucar.edu/wrf/users/namelist\\_best\\_prac\\_wrf.html](https://www2.mmm.ucar.edu/wrf/users/namelist_best_prac_wrf.html). accessed on 17 June 2023.

- National Center for Atmospheric Research, 2021. WRF Model Physics Options and References. University Corporation for Atmospheric Research. [https://www2.mmm.ucar.edu/wrf/users/physics/phys\\_references.html](https://www2.mmm.ucar.edu/wrf/users/physics/phys_references.html). accessed on 16 June 2023.
- National Center for Atmospheric Research, 2023. Urban Canopy Model. University Corporation for Atmospheric Research. <https://ral.ucar.edu/model/urban-canopy-model>. accessed on 5 July 2023.
- Ochoa-Rodríguez, S., Wang, L.P., Gires, A., Pina, R.D., Reinoso-Rondinel, R., Bruni, G., Ichiba, A., Gaitan, S., Cristiano, E., van Assel, J., Kroll, S., 2015. Impact of spatial and temporal resolution of rainfall inputs on urban hydrodynamic modelling outputs: a multi-catchment investigation. *J. Hydrol.* 531, 389–407.
- Opio, R., Sabiiti, G., Nimusima, A., Mugume, I., Sansa-Otim, J., 2020. WRF simulations of extreme rainfall over Uganda's Lake Victoria Basin: sensitivity to parameterization, model resolution and domain size. *J. Geosci. Environ. Protect.* 8 (4), 18–31.
- Pachauri, R.K., Meyer, L.A., Plattner, G.K., Stocker, T., 2014. Synthesis report. In: Contribution of Working Groups I, II and III to the Fifth Assessment Report of the Intergovernmental Panel on Climate Change. Intergovernmental Panel on Climate Change, Geneva, Switzerland.
- Pal, S., Dominguez, F., Dillon, M.E., Alvarez, J., Garcia, C.M., Nesbitt, S.W., Gochis, D., 2021. Hydrometeorological observations and modeling of an extreme rainfall event using WRF and WRF-hydro during the RELAMPAGO field campaign in Argentina. *J. Hydrometeorol.* 22 (2), 331–351.
- Patel, P., Thakur, P.K., Aggarwal, S.P., Garg, V., Dhote, P.R., Nikam, B.R., Swain, S., Al-Ansari, N., 2022. Revisiting 2013 Uttarakhand flash floods through hydrological evaluation of precipitation data sources and morphometric prioritization. *Geomat. Nat. Haz. Risk* 13 (1), 646–666.
- Pfahl, S., O'Gorman, P.A., Fischer, E.M., 2017. Understanding the regional pattern of projected future changes in extreme precipitation. *Nat. Clim. Chang.* 7 (6), 423–427.
- Powers, J.G., Klemp, J.B., Skamarock, W.C., Davis, C.A., Dudhia, J., Gill, D.O., Coen, J.L., Gochis, D.J., Ahmadov, R., Peckham, S.E., Grell, G.A., 2017. The weather research and forecasting model: overview, system efforts, and future directions. *Bull. Am. Meteorol. Soc.* 98 (8), 1717–1737.
- Qian, J.H., Zubair, L., 2010. The effect of grid spacing and domain size on the quality of ensemble regional climate downscaling over South Asia during the northeasterly monsoon. *Mon. Weather Rev.* 138 (7), 2780–2802.
- Reda, K.W., Liu, X., Haile, G.G., Sun, S., Tang, Q., 2022. Hydrological evaluation of satellite and reanalysis-based rainfall estimates over the Upper Tekeze Basin, Ethiopia. *Hydrol. Res.* 53 (4), 584–604.
- Rummeler, T., Arnault, J., Gochis, D., Kunstmann, H., 2019. Role of lateral terrestrial water flow on the regional water cycle in a complex terrain region: investigation with a fully coupled model system. *J. Geophys. Res. Atmos.* 124 (2), 507–529.
- Salamanca, F., Martilli, A., 2010. A new building energy model coupled with an urban canopy parameterization for urban climate simulations—Part II. Validation with one dimension off-line simulations. *Theor. Appl. Climatol.* 99 (3), 345–356.
- Schneider, L., Barthlott, C., Barrett, A.I., Hoose, C., 2018. The precipitation response to variable terrain forcing over low mountain ranges in different weather regimes. *Q. J. R. Meteorol. Soc.* 144 (713), 970–989.
- Seth, A., Giorgi, F., 1998. The effects of domain choice on summer precipitation simulation and sensitivity in a regional climate model. *J. Clim.* 11 (10), 2698–2712.
- Seto, K.C., Güneralp, B., Hutya, L.R., 2012. Global forecasts of urban expansion to 2030 and direct impacts on biodiversity and carbon pools. *Proc. Natl. Acad. Sci.* 109 (40), 16083–16088.
- Shepherd, J.M., 2005. A review of current investigations of urban-induced rainfall and recommendations for the future. *Earth Interact.* 9 (12), 1–27.
- Shepherd, J.M., Pierce, H., Negri, A.J., 2002. Rainfall modification by major urban areas: observations from spaceborne rain radar on the TRMM satellite. *J. Appl. Meteorol. Climatol.* 41 (7), 689–701.
- Skamarock, W.C., Klemp, J.B., Dudhia, J., Gill, D.O., Barker, D.M., Duda, M.G., Huang, X.Y., Wang, W., Powers, J.G., 2008. A Description of the Advanced Research WRF Version 3 (NCAR Tech. Note NCAR/TN-475+STR). National Center for Atmospheric Research, Boulder, CO, p. 113.
- Sofokleous, I., Bruggeman, A., Michaelides, S., Hadjinicolaou, P., Zittis, G., Camera, C., 2021. Comprehensive methodology for the evaluation of high-resolution WRF Multiphysics precipitation simulations for small, topographically complex domains. *J. Hydrometeorol.* 22 (5), 1169–1186.
- Stocker, 2014. Climate Change 2013: The Physical Science Basis: Working Group I Contribution to the Fifth Assessment Report of the Intergovernmental Panel on Climate Change, T. ed. Cambridge University Press.
- Sun, J., Ao, J., 2013. Changes in precipitation and extreme precipitation in a warming environment in China. *Chin. Sci. Bull.* 58, 1395–1401.
- Tarek, M., Brissette, F.P., Arsenault, R., 2020. Evaluation of the ERA5 reanalysis as a potential reference dataset for hydrological modelling over North America. *Hydrol. Earth Syst. Sci.* 24 (5), 2527–2544.
- Tewari, M., Chen, F., Wang, W., Dudhia, J., LeMone, M.A., Mitchell, K., Ek, M., Gayno, G., Wegiel, J., Cuenca, R.H., 2004. Implementation and verification of the unified NOAA land surface model in the WRF model. In: In 20th conference on weather analysis and forecasting/16th conference on numerical weather prediction, 1115th, pp. 2165–2170, 6.
- Thompson, G., Field, P.R., Rasmussen, R.M., Hall, W.D., 2008. Explicit forecasts of winter precipitation using an improved bulk microphysics scheme. Part II: Implementation of a new snow parameterization. *Monthly Weather Review* 136 (12), 5095–5115.
- Urbanobservatory, 2016. urban observatory. University of Newcastle upon Tyne, <https://urbanobservatory.ac.uk/>, accessed on 4 June 2023.
- UK Met Office, 2003a, Met Office Rain Radar Data from the NIMROD System. NCAS British Atmospheric Data Centre, <http://catalogue.ceda.ac.uk/uuid/82adec1f896af6169112d09cc1174499>, accessed on 15 June 2023.
- UK Met Office, 2003b, 1 km Resolution UK Composite Rainfall Data from the Met Office Nimrod System. NCAS British Atmospheric Data Centre, <https://catalogue.ceda.ac.uk/uuid/27dd6ffba67f667a18c62de5c3456350>, accessed on 15 June 2023.
- Vanden Broucke, S., Wouters, H., Demuzere, M., van Lipzig, N.P., 2019. The influence of convection-permitting regional climate modeling on future projections of extreme precipitation: dependency on topography and timescale. *Clim. Dyn.* 52, 5303–5324.
- Wang, W., Gill, D., 2012. WRF Nesting. National Oceanic and Atmospheric Administration. [https://ruc.noaa.gov/wrf/wrf-chem/wrf\\_tutorial\\_2012\\_brazil/WRF\\_nesting.pdf](https://ruc.noaa.gov/wrf/wrf-chem/wrf_tutorial_2012_brazil/WRF_nesting.pdf) (accessed on 8 June 2023).
- Wang, X., Steinle, P., Seed, A., Xiao, Y., 2016. The sensitivity of heavy precipitation to horizontal resolution, domain size, and rain rate assimilation: case studies with a convection-permitting model. *Adv. Meteorol.* 2016.
- Wang, W., Liu, J., Xu, B., Li, C., Liu, Y., Yu, F., 2022. A WRF/WRF-hydro coupling system with an improved structure for rainfall-runoff simulation with mixed runoff generation mechanism. *J. Hydrol.* 612, 128049.
- Warner, T.T., Peterson, R.A., Treadon, R.E., 1997. A tutorial on lateral boundary conditions as a basic and potentially serious limitation to regional numerical weather prediction. *Bull. Am. Meteorol. Soc.* 78 (11), 2599–2618.
- Weather Com, 2024. Rip Currents Danger Coast. The Weather Company, LLC. <https://weather.com/>. accessed on 19 August 2024.
- Weather Online Historical Data, 2023. Weather Online. WeatherOnline Ltd. - Meteorological Services. <https://www.weatheronline.co.uk/>. accessed on 19 August 2024.
- Weather Underground, 2024. Weather Underground. The Weather Company, LLC. <https://www.wunderground.com/>. accessed on 19 August 2024.
- Wikimedia Foundation, 2022. Newcastle upon Tyne. Wikipedia. [https://en.wikipedia.org/wiki/Newcastle\\_upon\\_Tyne](https://en.wikipedia.org/wiki/Newcastle_upon_Tyne). accessed on 4 June 2023.
- Xie, Y., Wang, J., 2021. Preliminary study on the deviation and cause of precipitation prediction of GRAPES kilometer scale model in southwest complex terrain area. *Acta Meteor. Sin.* 79 (5), 732–749.
- Xie, S.P., Deser, C., Vecchi, G.A., Collins, M., Delworth, T.L., Hall, A., Hawkins, E., Johnson, N.C., Cassou, C., Giannini, A., Watanabe, M., 2015. Towards predictive understanding of regional climate change. *Nat. Clim. Chang.* 5 (10), 921–930.
- Xu, J., Gao, Y., Chen, D., Xiao, L., Ou, T., 2017. Evaluation of global climate models for downscaling applications centred over the Tibetan Plateau. *Int. J. Climatol.* 37 (2), 657–671.
- Yu, Z., Wu, M., Min, J., Yan, Y., Lou, X., 2022. Impacts of WRF model domain size on meiyu rainfall forecasts over Zhejiang, China. *Asia-Pac. J. Atmos. Sci.* 58 (2), 265–280.
- Zhang, W., Villari, G., Vecchi, G.A., Smith, J.A., 2018. Urbanization exacerbated the rainfall and flooding caused by hurricane Harvey in Houston. *Nature* 563 (7731), 384–388.